ncl-1 Is Required for the Regulation of Cell Size and Ribosomal RNA Synthesis in *Caenorhabditis elegans*

Deborah J. Frank and Mark B. Roth

Division of Basic Sciences and Molecular and Cellular Biology Program, Fred Hutchinson Cancer Research Center, Seattle, Washington 98109

Abstract. Regulation of ribosome synthesis is an essential aspect of growth control. Thus far, little is known about the factors that control and coordinate these processes. We show here that the *Caenorhabditis elegans* gene *ncl-1* encodes a zinc finger protein and may be a repressor of RNA polymerase I and III transcription and an inhibitor of cell growth. Loss of function mutations in *ncl-1*, previously shown to result in enlarged nucleoli, result in increased rates of rRNA and 5S RNA transcription and enlarged cells. Furthermore, *ncl-1* adult worms are larger, have more protein, and have twice as much rRNA as wild-type worms. Localization studies show that the level of NCL-1 protein is independently regulated in different cells of the embryo. In wild-type embryos, cells with the largest nucleoli have the lowest level of NCL-1 protein. Based on these results we propose that *ncl-1* is a repressor of ribosome synthesis and cell growth.

During the life cycle of metazoans, growth occurs by increases in both the size of individual cells and in the actual number of cells. Most often these two processes are coordinated; cells are born at a certain size, double in size during the cell cycle, and then divide (Prescott, 1976). In some cases, however, cell size increase and cell division occur independently, as in early embryogenesis of many organisms where rapid cleavage divisions occur without any increase in cell size (Wilson, 1896). Similarly, growth of individual cells can occur in the absence of cell division. For instance, many adult tissues such as cardiac muscle increase in mass by cell size increase, or hypertrophy, rather than by cell division (Rakusan, 1984). A striking example of growth without division is during amphibian oocyte development (Dumont, 1972). Furthermore, an increase in cell size independent of cell division may also account for the fact that distinct cell types having identical DNA content can vary greatly in size within an individual organism (Altman and Katz, 1976).

Previous studies in bacteria and yeast have demonstrated that cell growth (increase in cell size and number) is tightly coupled to an increase in both protein synthesis and ribosome biogenesis (for review see Nomura et al., 1984). In higher eukaryotes, this correlation is seen in the diminished transcription of ribosomal RNAs (rRNA and 5S RNA) during quiescence and the subsequent increase after stimulation with growth factors (Johnson et al., 1974). Cell division is not a requirement for this coordination, however, as studies of hypertrophy in vertebrate cardiomyocytes also link rRNA and 5S RNA synthesis with control of cell size (McDermott et al., 1989). These studies suggest that regulators of ribosome synthesis may play an important role in cellular growth control. One gene that appears to function in the control of cell growth is the Retinoblastoma gene (Rb).[1] In addition to its role in the control of cell division, Rb has been shown to inhibit the synthesis of both rRNA and 5S RNA (Cavanaugh et al., 1995; White et al., 1996).

In eukaryotes, the nucleolus, the nuclear organelle in which rRNA synthesis and assembly of preribosomal subunits occurs (for review see Melese and Xue, 1995), is a good cytological marker of ribosome synthesis as the size of the nucleolus is indicative of the level of rRNA synthesis (Kurata et al., 1978; Altmann and Leblond, 1982; Moss and Stefanovsky, 1995). Interestingly, tumor cells not only exhibit rapid cell growth and division, but also often have enlarged nucleoli (Busch and Smetana, 1970; Derenzini and Trere, 1991). Similarly, during both normal developmental cardiac hypertrophy and aberrant hypertrophy that occurs in many forms of heart disease, nucleoli are enlarged (Hatt et al., 1978; Cluzeaud et al., 1984; Dalen et al., 1987). Enlarged nucleoli have also been observed in the *ncl-1* mutant of the nematode *Caenorhabditis elegans* (Hedgecock and Herman, 1995). We have isolated the *ncl-1*

Address all correspondence to Mark B. Roth, Fred Hutchinson Cancer Research Center, 1100 Fairview Ave., N Mailstop A3-013, Seattle, WA 98109. Tel.: (206) 667-5602. Fax: (206) 667-6877. E-mail: mroth@fred.fhcrc.org

1. *Abbreviations used in this paper*: ITS, internal transcribed spacer; PML, promyelocytic leukemia; RAR, retinoic acid receptor; Rb, retinoblastoma gene; UTP, uridine 5′triphosphate.

gene and show that it appears to repress rRNA and 5S RNA synthesis and to be an inhibitor of both ribosome biosynthesis and cell growth.

Materials and Methods

Strains and Alleles

Bristol strain N2 was used as the standard wild-type strain. The *ncl-1* alleles used were: *e1865* (Hedgecock and Herman, 1995) and *e1942* (provided by C. Kenyon, University of California, San Francisco, CA). Both were outcrossed against N2 five times. *clr-1 (e1745)* was used for cell size analysis. Nematode strains were cultured as described by Brenner (1974).

Worm Size and Total Protein Measurements

Two-dimensional images of wild-type and *ncl-1 (e1942)* worms grown for 50 h at 20°C after hatching were collected using a charge-coupled device camera and National Institutes of Health (NIH) image. Worm sizes were determined in Canvas (Deneba Software, Miami, FL) and then analyzed in Microsoft Excel (Redmond, WA). The amount of total protein was determined for wild-type and *ncl-1 (e1942)* adult worms grown at 20°C for 44 h after hatching using the Amidoschwarz assay (Schaffner and Weissmann, 1973). Total DNA in each sample was determined using a fluorometer (model TKO-100; Hoefer Scientific Instruments, San Francisco, CA). Analysis of total protein to DNA ratios and statistics was performed using Microsoft Excel.

In Situ Hybridization

In situ hybridization using either 5.8S or internal transcribed spacer (ITS)2 probes was done according to the method of Seydoux and Fire (1994). The 5.8S (GGAGGCCCAGTTGGTGCTATGCGTTCG) and ITS2 (CAAGTCGGACGCCATTTGGCAGCTCCTCCG) antisense oligo probes were directed against nucleotides 2204–2230 and 2426–2455, respectively, of the *C. elegans* rDNA repeat (Ellis et al., 1986). Probes were end labeled with terminal deoxynucleotidyl transferase and digoxigenin–ddUTP (Boehringer Mannheim Biochemicals, Indianapolis, IN) and then used at a concentration of 1.0 μg/ml in 7.7% formamide, 2× SSC hybridization buffer. Probes were then visualized using FITC-conjugated anti-digoxigenin antibodies (Boehringer Mannheim Biochemicals). The following controls for specificity of hybridization were performed: an anti-SL1 (spliced leader) probe (CTCAAACTTGGGTAATTAAACC) hybridized to the cytoplasm of all cells and to cytoplasmic granules in the P cells as previously described (Seydoux and Fire, 1994), but did not hybridize to nucleoli; and prehybridizing of slides with 20 μg/ml of unlabeled 5.8S or ITS2 antisense oligo inhibited hybridization with the respective labeled oligos.

Run-on Transcription Assays

Extracts were prepared from early embryos (95% earlier than 100-cell stage) by collecting and bleaching worms from the different genetic backgrounds just as they began to become gravid and contained <10 embryos per hermaphrodite. Preparation of extracts for transcription assays and quantitation of DNA in the extracts was done as described (Schauer and Wood, 1990), except that salmon sperm DNA was used to provide a standard curve and a fluorometer (model TKO-100; Hoefer Scientific Instruments) was used.

For some experiments, run-on transcription reactions and hybridizations were performed as described (Schauer and Wood, 1990), except that volumes of embryonic extracts corresponding to 50 μg of DNA, 100 μCi of [^{32}P]uridine 5′-triphosphate (UTP), 2 mM ATP, 2 mM CTP, 2 mM GTP, and 0.05 mM cold UTP were used in 100-μl reactions and then hybridizations were done for 2 d at 42°C. In other experiments, the reaction conditions were as follows: volumes of extract corresponding to 2.5 μg of DNA were incubated in buffer containing 5 mM Tris-HCl, pH 8.0, 2.5 mM $MgCl_2$, 150 mM KCl, 100 μCi [^{32}P] cytosine 5′-triphosphate (CTP), 0.8 mM ATP, 0.8 mM GTP, 0.8 mM UTP, 1 mM DTT, and 200 U/ml RNAsin (Promega Corp., Madison, WI) (final volume was 20 μl) for 30 min at room temperature. For these experiments, hybridization was performed for 18 h at 65°C in 10 mM TES (Sigma Chemical Co., St. Louis, MO) pH 7.5, 1% SDS, 10 mM EDTA, 250 μg/ml *Escherichia coli* RNA, 300 mM NaCl, 100× Denhardt's (2% Ficoll 400, 2% polyvinylpyrrolidone, 2% bovine serum albumin), and 0.25% powdered nonfat milk. In each experiment, three reactions were performed for each genotype tested.

Slot blot filters were prepared as follows: for each reaction performed, 5 μg of each of the DNAs of interest were denatured in 0.3 M NaOH at 65°C for 10 min and then neutralized by the addition of 1 vol of 2 M ammonium acetate. Denatured DNAs were loaded onto Gene Screen Plus membrane (DuPont-NEN, Boston, MA), presoaked in 1× SSC, 10 mM Tris, pH 7.4, using a slot blotting apparatus (Schleicher & Schuell, Inc., Keene, NH). DNAs of interest were as follows: rDNA was pCe7 (Files and Hirsh, 1981); 5S RNA gene construct was made by cloning a 160-bp StuI-HindIII fragment of plasmid 985(Sl1/5S) (Ferguson et al., 1996) into Bluescript KS+ (Stratagene, La Jolla, CA) cut with EcoRV and HindIII; histone genes were in clone pCeh-3 (Roberts et al., 1989). Quantitation of hybridization signals was performed using a phosphorimager (Molecular Dynamics, Sunnyvale, CA) and data from all experiments performed (four experiments for wild-type and *ncl-1 [e1865]* on rDNA and 5S; two experiments for *ncl-1 [e1942]* on rDNA, 5S, and histones, and wild-type and *ncl-1 [e1865]* on histones) were collated for the graphs presented in Fig. 3.

Northern Blot Analysis

Northern blots were performed as described in Ausubel et al. (1987). The 28S rRNA (CTGCACTGACGGAAGCTCCAGCCGAGCC) antisense oligo probe was directed against nucleotides 4113–4140 of the *C. elegans* rDNA repeat (Ellis et al., 1986). The histone (AGAGGGCCGTTGGGTTCGGT) antisense oligo probe was directed against the conserved 3′ sequence in all *C. elegans* histone messages (Roberts et al., 1989).

Cloning of ncl-1

The *ncl-1* locus was identified through a series of germline transformation experiments with cosmids and subclones of cosmid ZK112. DNA was injected with the dominant marker *rol-6* (Mello et al., 1991) into the syncytial gonad of *ncl-1 (e1865)* or *ncl-1 (e1942)* animals. DNA was injected at a final concentration of 0.1 mg/ml. Adult Rol progeny were analyzed by differential interference contrast microscopy for rescue of the Ncl phenotype. Partial rescue (not all cells were rescued) was obtained with the 7.5-kb rescuing fragment (pZK112-1b).

Antisense RNA derived from a 1-kb HindIII-XhoI fragment of pZK112-1b was injected into the syncytial gonad of wild-type hermaphrodites according to the procedure of Guo and Kemphues (1995). These worms gave progeny with enlarged nucleoli, indicative of *ncl-1* phenocopy.

A full-length *ncl-1* cDNA was obtained by screening a *C. elegans* mixed stage library (Stratagene) with the 1-kb HindIII-XhoI fragment of pZK112-1b. Sequencing of this cDNA revealed the same exon boundaries as predicted by GeneFinder. This cDNA begins at a position 134-bp upstream of the first ATG and terminates with a poly A tail 1,355-bp downstream of the first in-frame stop codon. The Matcher program (Fischetti et al., 1993) was used to identify the predicted coiled-coil motif in NCL-1. Sequence data is available under EMBL/GenBank/DDBJ accession number AF047027.

Production of Monoclonal Antibody, Immunoblotting, and Immunostaining

The pET-16b vector (Novagen Inc., Madison, WI) was used to generate a protein fusion between the 10-His tag and amino acids 24–377 of NCL-1. The bacterially expressed fusion protein 10-His–NCL was purified by chromatography on Ni^{2+}-NTA-Agarose (QIAGEN Inc., Santa Clarita, CA). mAb D3C2 and ascites fluid were generated as described by Harlow and Lane (1988).

For immunoblotting, embryo extracts prepared by overnight extraction of embryos in *N*,*N*-dimethylformamide (Sigma Chemical Co.) followed by sonication of insoluble material in NEST-2 (5% SDS, 20 mM EDTA, 50 mM Tris-HCl, pH 6.8) were run on 6% SDS–polyacrylamide gels and then transferred to nitrocellulose. Blots were stained with Ponceau S, blocked for 1 h in 3% BSA and 10% nonfat dry milk in TBST (50 mM Tris-Hcl, pH 8.0, 150 mM NaCl, 0.05% Tween 20), incubated overnight at room temperature in primary antibody, washed in TBST, incubated in horseradish peroxidase-linked anti–mouse Ig (Amersham Corp., Arlington Heights, IL) diluted 1:2,500 in 3% BSA in TBST, washed extensively in TBST, and then processed for detection using the SuperSignal Substrate, Western blotting kit (Pierce Chemical Co., Rockford, IL). mAb D3C2 was used as undiluted hybridoma supernatant.

Fixation of embryos was as described (Albertson, 1984) with the following exceptions. Slides were pretreated with 3-aminopropyltriethoxysilane (Sigma Chemical Co.) and fixation was then done in *N*,*N*-dimethylformamide at −20°C for 5 min. Gonad fixation and staining was performed in solution. For immunostaining, mAb D3C2 ascites fluid was used at a 1:500 dilution. mAb K121 against 2,2,7-trimethylguanosine (Oncogene Science, Inc., Manhasset, NY) was used at a 1:50 dilution.

Results

Increased Nucleolar and Cellular Size in ncl-1 Mutants

To begin to investigate the mechanisms regulating cell growth and ribosome synthesis, we have focused on the gene *ncl-1* in *C. elegans. ncl-1 (e1865)* and *ncl-1 (e1942)* have previously been described as recessive mutations that result in enlarged nucleoli that can be detected by Nomarski microscopy in nearly all cells of live worms (Hedgecock and Herman, 1995). Both alleles are recessive and appear genetically to be loss of function mutations. This phenotype is fully penetrant in both alleles and is especially evident in embryos. For example, nucleoli are clearly detectable in a *ncl-1* four-cell embryo but are not visible in a wild-type four-cell embryo (Fig. 1). In larvae and adult worms, enlarged nucleoli can be seen in all cells with the exception of the gut and syncytial gonad since these tissues have large nucleoli in wild type. Similarly, the degree to which nucleolar size changes in the mutant differs in distinct cell types; the small or not detectable nucleoli of some wild-type cells are clearly enlarged in *ncl-1* mutants, whereas the large nucleoli of other cells are only slightly enlarged in *ncl-1* mutants.

In addition to enlarged nucleoli, *ncl-1* mutants also exhibit increases in growth. By microscopic imaging and measurement of worms in two dimensions, we observed that adult *ncl-1 (e1942)* worms are 9% larger than wild-type worms at identical times after hatching ($n = 20$ for each, $P < 0.01$). Previous studies have shown that there is no difference in cell division timing or final number of cells between *ncl-1* mutants and wild type (Hedgecock and Herman, 1995). The enlarged size of *ncl-1* mutants, therefore, is likely due to increased cell sizes. To test this, we used Nomarski microscopic imaging of live worms to analyze the sizes of specific cells and found that some cells in *ncl-1* mutants are larger than the respective cells in wild-type worms. To quantitate the size increase, we made use of the mutant *clr-1*; these mutant worms are clear when shifted to the nonpermissive temperature, thereby allowing cell outlines to be visualized and cell sizes to be measured (Kipreos et al., 1996). We made two-dimensional measurements of specific cells and compared their sizes between *clr-1* and *ncl-1 (e1942)*;*clr-1* larvae at identical times after hatching. The cell anterior lateral microtubule (ALM) is 47–78% larger in *ncl-1*;*clr-1* than in *clr-1*, and the cell Q2.pap is 75–126% larger (Table I). The evidence that the *ncl-1* gene product functions in these two cells is that they both have enlarged nucleoli in *ncl-1* and *ncl-1*;*clr-1* worms (data not shown), and that *ncl-1* is known to function cell autonomously (Hedgecock and Herman, 1995). These results demonstrate that *ncl-1* mutants have larger cells than wild-type worms and suggest that the *ncl-1* gene product represses cell growth.

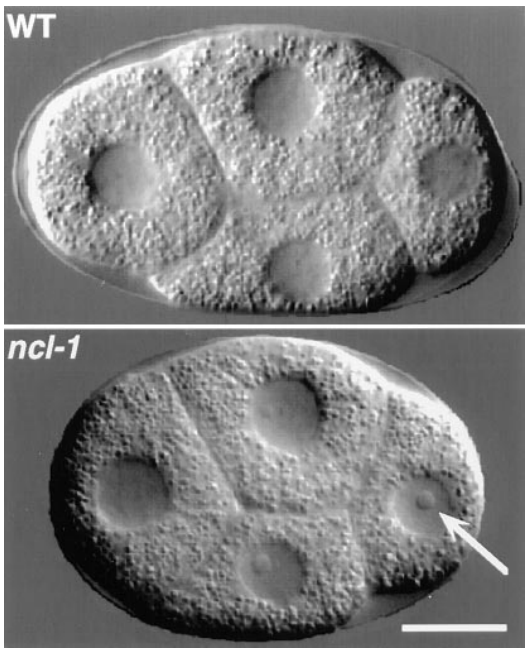

Figure 1. Nucleoli are visible in *ncl-1* but not wild-type early embryos. Live wild-type and *ncl-1* four-cell embryos were visualized using differential interference contrast microscopy. One or two nucleoli can be seen in all nuclei of *ncl-1* embryos; in this image nucleoli in the most anterior blastomere are out of the plane of focus. The nucleolus in the most posterior blastomere is indicated with an arrow. In this and all other figures, anterior is to the left and dorsal is up. Bar, 10 μm.

Increased Protein and rRNA in ncl-1 Mutants

Because an increase in cell size is likely to indicate increased protein synthesis, we assayed protein levels in wild-type and mutant worms and found that adult *ncl-1 (e1942)* worms have 22% more protein than wild-type worms ($n = 10$ for each, $P < 0.0005$). Because this increased level of protein in *ncl-1* worms may indicate an increased capacity for protein synthesis, or more ribosomes, and because *ncl-1* mutants have enlarged nucleoli, we hypothesized that *ncl-1* mutant worms might have an increased amount of ribosomal RNA. To quantitate steady-state rRNA, we performed Northern blots on RNA from mutant and wild-type worms 48 h after hatching. We

Table I. Quantitative Comparison of Cell Sizes in clr-1 and ncl-1; clr-1 Worms

Cell	*clr-1*	*ncl-1*; *clr-1*	*P* value	Area increase	Vol increase
ALM	49 ± 5 (12)	72 ± 9 (7)	<0.0005	1.47	1.78
Q2.pap	25 ± 2 (9)	43 ± 10 (8)	<0.001	1.75	2.26

To quantitatively determine the effect that *ncl-1* has on cell size, we compared cell sizes in *clr-1* with those in *ncl-1*; *clr-1* worms. Worms were raised for 49 h after hatching at 20°C and then were shifted to 26°C for 4 h. Nomarski images of particular cells were captured so that the focal plane in which the cell was largest was analyzed. Images were collected using a charge-coupled device camera and NIH image. Cell sizes were then determined in Canvas and were analyzed in Microsoft Excel. Cell sizes are presented in arbitrary units as the mean and standard deviation. The number of each type of cell analyzed is denoted in parentheses. The calculated fold increase in area may be an underestimate of the increase in cell size, whereas the fold increase in volume may be an overestimate as the calculation assumes the cells are perfect spheres.

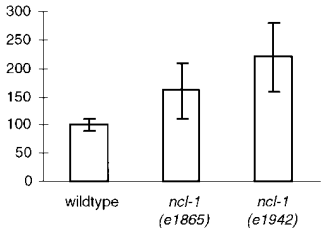

Figure 2. Increased steady-state level of rRNA in *ncl-1* mutants. RNA was isolated from three samples each of wild-type, *ncl-1 (e1865)*, and *ncl-1 (e1942)* worms grown at 20°C for 48 h after hatching. RNA was run on a 1% agarose formaldehyde gel and then transferred to nitrocellulose. The same blot was hybridized with both histone and 28S rRNA probes. The graph represents relative levels of 28S rRNA standardized to histone message. Quantitation was performed with a phosphorimager. This experiment was performed twice with similar outcomes; the data from one experiment is presented here. Error bars represent standard deviations.

found that the ratio of histone mRNA to total DNA is the same in *ncl-1* and wild-type worms at identical times after hatching, and therefore standardized the 28S rRNA hybridization signal to the histone message on the same blot. We found that *ncl-1 (e1865)* adults contain 1.6 times more rRNA than wild-type worms ($P < 0.05$) and that *ncl-1 (e1942)* adults contain 2.2 times more rRNA than wild-type worms ($P < 0.05$) (Fig. 2). Thus, one way in which the *ncl-1* gene product could restrict cell size is by repression of the steady-state level of rRNA and, therefore, the capacity for protein synthesis.

Increased RNA Polymerase I and III Transcription in ncl-1 Mutants

We next considered the possibility that the increased amount of rRNA in *ncl-1* mutants is due to an increase in the rate of rRNA transcription. To test this hypothesis, we compared the level of rRNA present in the nuclei of early wild-type and *ncl-1* embryos by in situ hybridization. Although we detected 5.8S rRNA in the cytoplasm in both wild-type and *ncl-1* embryos, hybridization in the nucleus was higher in *ncl-1* embryos than in wild-type (Fig. 3, *a* and *b*). In all *ncl-1* embryos examined, nuclear hybridization was seen in one or two sites that overlapped with the sites of visible nucleoli, whereas this pattern was not seen in any of the wild-type embryos examined (Fig. 3 *b*). To distinguish between precursor and mature rRNA, we next performed in situ hybridizations using an oligo probe directed against ITS2 that is present in precursor rRNA but is removed during processing (Perry, 1976). No signal was detected in the cytoplasm of either wild-type or *ncl-1* embryos using this probe. In the nucleus, hybridization was much stronger in *ncl-1* than in wild-type embryos (Fig. 3, *e* and *f*). Similar to the 5.8S probe, we detected one or two sites of hybridization that colocalize with nucleoli in nuclei of all *ncl-1* embryos examined (Fig. 3 *f*) This was not seen in any of the wild-type embryos examined. These data indicate that in *ncl-1* embryos, there is an increase in the level of precursor rRNA present in the nucleus.

To determine if this increase in level of precursor rRNA in the nucleus is due to an increase in the rate of rRNA transcription in mutant embryos, we performed nuclear run-on assays on wild-type and mutant embryos (refer to Materials and Methods). We analyzed early embryos be-

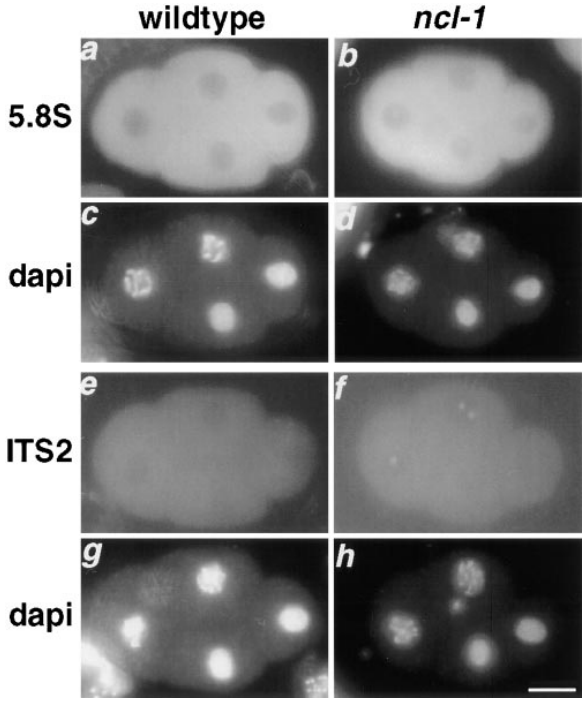

Figure 3. Increased nuclear precursor rRNA in *ncl-1* mutants. Wild-type (*a*, *c*, *e*, and *g*) and *ncl-1* (*b*, *d*, *f*, and *h*) embryos were hybridized to 5.8S (*a* and *b*) or ITS2 (*e* and *f*) digoxigenin-labeled antisense oligo probes. Probes were visualized using an anti-digoxigenin antibody coupled to FITC. DNA was visualized by staining with 4′,6-diamidino-2-phenylindole (DAPI) (*c*, *d*, *g*, and *h* correspond to *a*, *b*, *e*, and *f* respectively). In *ncl-1*, nucleoli are detectable with both the 5.8S probe (*b*) which detects both precursor and mature rRNA, and the ITS2 probe (*f*) which detects only unprocessed precursor rRNA. Bar, 10 μm.

cause at this time in development there is a very clear difference between the size of nucleoli in mutant and wild-type (refer to Fig. 1). Nuclear run-on assays were performed on equivalent numbers of nuclei from mutant and wild-type extracts as determined by standardization to DNA by fluorometry. We first analyzed rRNA transcription by hybridization of nascent RNA labeled in the run-on reaction to DNA corresponding to one repeat of *C. elegans* rDNA. We found that the rate of rRNA transcription is 2–2.5 times higher in *ncl-1* early embryos than in wild-type embryos (Fig. 4 *a*). This observation suggests that, as hypothesized by Hedgecock and Herman (1995), the *ncl-1* gene product represses rRNA transcription, and that *ncl-1* worms have enlarged nucleoli because of increased nucleolar activity.

To address the polymerase specificity of the *ncl-1* phenotype, we assayed RNA polymerase II and III transcription using the nuclear run-on assay. To detect RNA polymerase III transcription, we hybridized radiolabeled nascent RNA to DNA encoding the *C. elegans* 5S gene. RNA polymerase II transcription was detected by hybridization of radiolabeled nascent RNA to DNA encoding the histone H2A, H2B, H3, and H4 genes. We found that 5S transcription was approximately twofold higher in *ncl-1* than in wild-type embryos (Fig. 4 *b*), whereas histone transcription was not significantly affected (Fig. 4 *c*). These data indicate that the *ncl-1* gene product functions to mod-

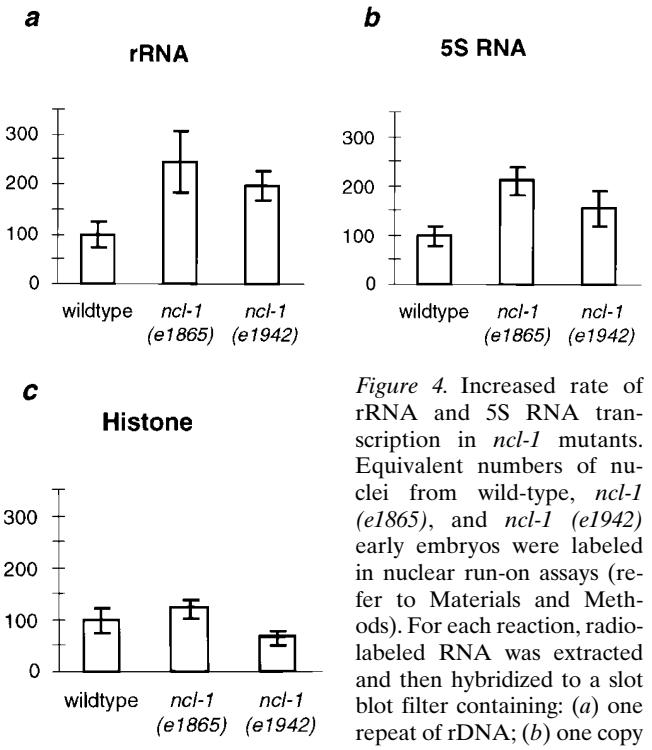

Figure 4. Increased rate of rRNA and 5S RNA transcription in *ncl-1* mutants. Equivalent numbers of nuclei from wild-type, *ncl-1 (e1865)*, and *ncl-1 (e1942)* early embryos were labeled in nuclear run-on assays (refer to Materials and Methods). For each reaction, radiolabeled RNA was extracted and then hybridized to a slot blot filter containing: (*a*) one repeat of rDNA; (*b*) one copy of 5S RNA; or (*c*) one copy each of histones H2A, H2B, H3, and H4. In each case, graphs represent a minimum of two independent nuclei preparations and three reactions per preparation. The y axis represents percentages with wild-type set to 100. Quantitation was performed with a phosphorimager. Error bars represent standard deviations. The probability (*P*) that the mutants are different than wild-type is as follows: *ncl-1 (e1865)* rRNA, $P < 0.005$; *ncl-1 (e1942)* rRNA, $P < 0.02$; *ncl-1 (e1865)* 5S RNA, $P < 0.001$; *ncl-1 (e1942)* 5S RNA, $P < 0.2$; *ncl-1 (e1865)* histone, $P < 0.5$; *ncl-1 (e1942)*, $P < 0.5$.

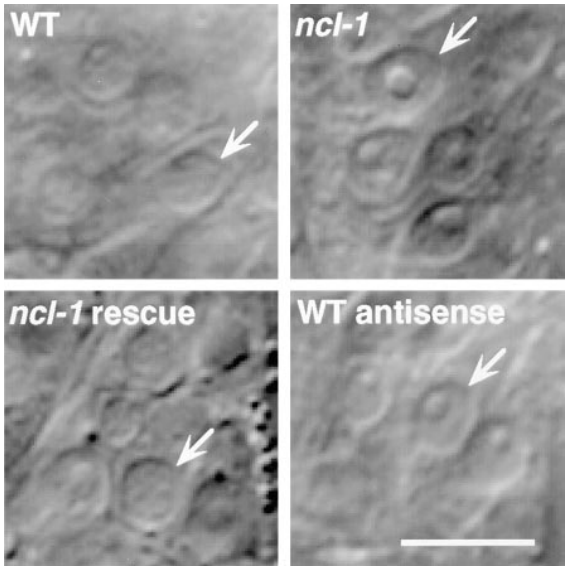

Figure 5. Rescue and antisense phenocopy of *ncl-1*. Each image shows a region of a worm anterior of the posterior bulb of the pharynx. Nuclei of neurons in this region are indicated with arrows. In wild type, these nuclei have very small or no detectable nucleoli. In *ncl-1* worms, neuronal nuclei have large nucleoli. Injection of a 7.5-kb fragment of genomic DNA containing the *ncl-1* gene into the syncytial gonad of *ncl-1* worms results in partially rescued F1 progeny (*ncl-1 rescue*). These worms have neurons that do not have large nucleoli. Injection of antisense RNA from the *ncl-1* gene into the syncytial gonad of wild-type worms results in phenocopy in F1 progeny (*WT antisense*). Neurons in these wild-type worms have enlarged nucleoli. Bar, 10 μm.

ulate both RNA polymerase I (rRNA) and RNA polymerase III (5S) transcription, whereas it does not appear to play a general role in the regulation of RNA polymerase II transcription. This suggests that *ncl-1* may repress the production of ribosomes, and thus the capacity for protein synthesis, through inhibition of RNA polymerase I and III transcription.

NCL-1 Is a B Box Zinc Finger Protein

ncl-1 had previously been localized to cosmid C33C3 by transformation rescue (Miller et al., 1996). We achieved rescue with the neighboring cosmid ZK112, which has been sequenced by the *C. elegans* genome consortium (Sulston et al., 1992). Analysis of subclones from this cosmid resulted in identification of a 7.5-kb genomic fragment containing one predicted gene that partially rescued the *ncl-1* enlarged nucleolus phenotype (Fig. 5). To confirm that this gene is *ncl-1*, we injected antisense RNA transcribed from this genomic fragment into the syncytial gonad of wild-type hermaphrodites. This resulted in enlarged nucleoli in larval progeny (Fig. 5). In both the rescue and antisense experiments, the numbers of affected nuclei varied from animal to animal. These lines of evidence together indicate that this gene is *ncl-1*.

The *ncl-1* cDNA can encode an 851-amino acid protein (Fig. 6 *a*) with two zinc finger motifs previously described as B boxes (Reddy et al., 1992). It also contains a predicted coiled-coil motif. Proteins that share these motifs include the oncogenic proteins promyelocytic leukemia (PML), T18, and ret finger protein (RFP), as well as other proteins such as XNF7, SS-A/Ro, regulatory protein, T lymphocyte (RPT-1), and PwA33 (for review see Reddy et al., 1992). Although NCL-1 does not contain a really interesting new gene (RING) zinc finger motif common to many of these proteins, it is most like PML and T18 in that these proteins all have two B box zinc finger motifs. Outside of the B boxes and coiled-coil motif, there is no homology between NCL-1 and any other proteins.

Expression of NCL-1 Is Correlated with Repression of rRNA Synthesis and Decreased Cell Size in Wild-type Embryos

We were interested in learning the spatial and temporal expression of NCL-1 and therefore generated mouse polyclonal antisera and a mouse mAb against the amino-terminal half of NCL-1 (refer to Materials and Methods). Results with polyclonal antisera and the monoclonal antibody are identical; only those experiments using mAb D3C2 are presented here. mAb D3C2 recognizes two bands of ~100-kD in wild-type extracts, but not in extracts made from either of the two mutant alleles of *ncl-1* (Fig. 6 *b*). The upper band is a phosphorylated form of NCL-1 (data not shown). The predicted molecular weight of NCL-1 is

a

```
METQLSVQLGLDSLLTDFGLESVMNKQQQLFANMGLSDIGAPTPSTAIPV   50
PNAHLHPSMVAGSDPSNPVVGFGFGSPSSTTSSSPPLSNSPTIEQQQHAQ  100
LTAMMQGIMSNNNVAVSNGSGVQVASVPAVHCSGCKSNETATSFCQDCNA  150
NLCDNCTMAHKFMHCFADHRVVSLTTPGTGSSSSSTSSSSSASSTSSHQV  200
PSLGGKQSPDSMMLGSGKRSVLCLQHRASELVFFCVSCNLAICRDCTVSD  250
HPSGTHQYELIADVADKQMLKMEQLIADARSKHADMLDMFKQVDNKQQVL  300
TASLHNAHAQLEETVSNLINVIQDQKKTLAKDIDNAFAAKQIQLTMVDKR  350
IQSMADKLSQTIEFSRRLMSFASPAEVMVFKQLLDTRLQLFLGFNPDTSG  400
VLMTPCEIEYLGAAGLFNNSASTVSQLLGSVHGGSPINNAPAANDFLMPQ  450
AGLAPIGRAQSRIIPIEQNQLARSPPHHIAGSLPMNAYSDSNLLRPNKDF  500
GGSSQSLGPFNPLGASVPGAAADPFSSQYDKWSLGVEPSVGGLLEGGNVD  550
EEKFQTLFPPSRSQIKRQKMIYHCKFGEFGVMEGQFTEPSGVAVNGQGDI  600
VVADTNNHRIQVFDKEGRFKFQFGECGKRDGQLLYPNRVAVNRTTGDFVV  650
TERSPTHQIQVYNQYGQFLRKFGANILQHPRGVCVDSKGRIIVVECKVMR  700
VIIFDMFGNILQKFSCSRYLEFPNGVCTNDKNEILISDNRAHCIKVFSYE  750
GQYLRQIGGEGVTNYPIGVGINSLGEVVVADNHNNFNLTVFSQDGTMIGA  800
LESRVKHAQCFDVALVDDGSVVLASKDYRLYLYRFLPATSGQSTSSASSQ  850
I                                                    851
```

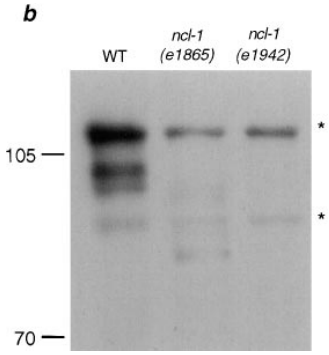

Figure 6. Predicted amino acid sequence and Western blot analysis of NCL-1. (*a*) A *ncl-1* cDNA cloned by hybridization to the rescuing genomic fragment confirmed the exon structure of the gene ZK112.2 predicted by the *C. elegans* genome consortium. The 851-amino acid open reading frame contains two B box zinc finger motifs (amino acids 132–164 and 223–256) that are shaded with conserved cysteines and histidines in bold. Predicted coiled-coil motif (amino acids 257–363, determined using the Matcher program) is underlined. The predicted molecular weight of NCL-1 is 92 kD. (*b*) Extracts of wild-type, *ncl-1 (e1865)*, and *ncl-1 (e1942)* embryos were run on a 6% SDS-PAGE gel, transferred to nitrocellulose, and then probed with mAb D3C2. Background bands detected without primary antibody are denoted by asterisks. mAb D3C2 recognizes two bands of ~97-kD in wild-type but not *ncl-1* extracts. No immunoreactive species is detected in extracts from *ncl-1(e1942)*, whereas a faster migrating species of ~80-kD is detected in extracts from *ncl-1 (e1865)* embryos.

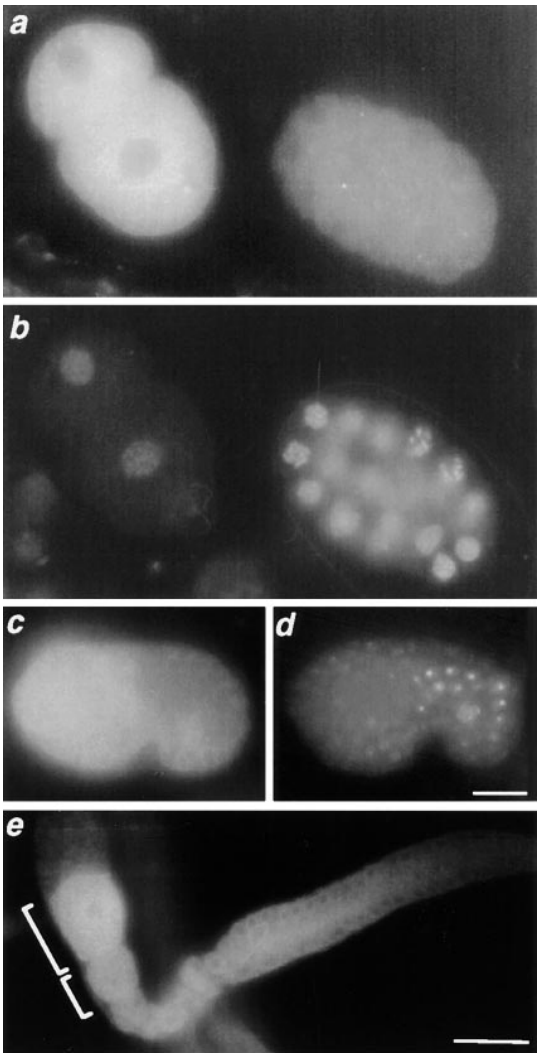

Figure 7. Localization of NCL-1 protein. (*a* and *b*) Immunofluorescence micrographs of wild-type embryos stained for NCL-1 protein with mAb D3C2 (*a*) and with DAPI to visualize nuclei (*b*). Intense staining is seen in the two-cell embryo (*left*), but is diminished by the 28-cell stage (*right*). (*c* and *d*) Immunofluorescence micrographs of two different wild-type 300-cell embryos stained with either mAb D3C2 to visualize NCL-1 protein (*c*) or with mAb K121 (*d*) to visualize nucleoli. At this stage, NCL-1 protein appears to be present in all cells except for those of the gut which have prominent nucleoli as detected by mAb K121. (*e*) Immunofluorescence micrograph of a wild-type gonad stained with mAb D3C2. Staining is most intense in the most mature oocyte (*left*). The large and small brackets indicate the most mature and second most mature oocytes, respectively. Bars, 10 μm.

92-kD. In *ncl-1(e1865)* embryo extracts, a faster migrating polypeptide of ~80-kD was detected, whereas no immunoreactive species was detected in extracts from *ncl-1 (e1942)*. These results confirm that this gene is *ncl-1* and suggest that *ncl-1(e1942)* is a protein-null allele, whereas *ncl-1(e1865)* produces a shorter form of the protein.

Given that NCL-1 appears to act as an inhibitor of RNA polymerase I transcription, and thus nucleolar size and function, we hypothesized that it would be expressed when nucleoli are absent, and not expressed when nucleoli are visible. We first examined early embryos in which nucleoli are not detectable in wild-type. Indirect immunofluorescence using mAb D3C2 showed that in wild-type embryos, NCL-1 is a cytoplasmic protein with no obvious nuclear accumulation. NCL-1 staining is abundant in early embryos and then rapidly diminishes during development (Fig. 7 *a*). We detect no staining with mAb D3C2 in *ncl-1 (e1942)* mutant embryos at any stage (data not shown).

We next assayed NCL-1 expression in 300-cell stage embryos, since nucleoli are first visible in some cells at this stage in development. As a marker for nucleoli in these cells, we stained similarly staged embryos with mAb K121 that recognizes nucleoli in *C. elegans* (Fig. 7 *d*). Immunostaining with mAb D3C2 showed that NCL-1 is present in the cytoplasm of all cells except those of the developing gut (Fig. 7 *c*); these cells are among the first to differentiate in the embryo, are the largest cells in the embryo, and have very large nucleoli. Lastly, we analyzed the NCL-1 staining pattern in the hermaphrodite gonad. Nucleoli are visible in the syncytial gonad of adult hermaphrodites but disappear as oocytes mature. We observed that cytoplas-

mic NCL-1 staining is absent in the mitotic region of the syncytial gonad, low in the meiotic region, and then increases throughout oocyte maturation such that the most intense staining is seen in the most mature oocyte (Fig. 7 *e*). Together these staining experiments indicate that NCL-1 protein is present in cells in which nucleoli are absent, and absent from large cells in which nucleoli are prominent. This suggests that the regulation of NCL-1 protein expression is important for the control of cell growth and ribosome synthesis.

Discussion

NCL-1, a Key Molecule in the Regulation of Cell Growth and Ribosome Synthesis

We have shown that the *C. elegans* gene *ncl-1* may inhibit ribosome synthesis and restrict cell growth. In *ncl-1* loss of function mutants, individual cells are larger than wild-type and as a result, the worms themselves are larger. In addition, we observed a twofold increase in steady-state amount of rRNA in *ncl-1* mutant worms relative to wild-type. As rRNA is very stable (for example, Liebhaber et al. [1978] reported a rRNA half-life of ⩾700 h in primary human fibroblasts), this increase is likely due to the 2–2.5 fold increase in the rate of rRNA transcription we observed in *ncl-1* mutant embryos relative to wild-type. We observed a similar effect on the rate of 5S RNA transcription. These results are consistent with those seen by others in systems in which rRNA or 5S RNA transcription are experimentally induced, such as by application of 12-*o*-tetradecanoylphorbol-13-acetate to cells (Allo et al., 1991; Garber et al., 1991; Vallett et al., 1993). Furthermore, since ribosomal RNA makes up 60–90% of cellular RNA, a twofold increase is a substantial alteration. This result suggests that *ncl-1* worms may have more ribosomes than wild-type worms, consistent with our finding that *ncl-1* worms contain more protein than wild-type worms. Therefore, the difference in cell size and whole animal size between *ncl-1* and wild-type worms may be accounted for by an increased ability to synthesize proteins.

The regulation of expression of NCL-1 protein appears to be important for the control of cell growth and ribosome synthesis as its abundance is inversely related to the presence of visible nucleoli, the nuclear organelles in which rRNA synthesis occurs. NCL-1 is present in the early embryo where nucleoli are not visible and high levels of zygotic rRNA production are perhaps not necessary because of the maternal contribution of ribosomes. At the 300-cell stage, NCL-1 protein is present in all cells except those of the gut. Gut cells are the first cells to differentiate in the embryo, are the largest cells in the embryo (Wood, 1988), and have large nucleoli. In addition to being very large, the gut cells are quite active metabolically (the gut produces all of the digestive enzymes as well as the yolk for the gonad; White, 1988) and therefore presumably require high levels of ribosome synthesis. Tissues with high metabolic activity, such as the gut, produce high levels of ribosomes as demonstrated in studies of *Drosophila* paragonial glands (Schmidt et al., 1985). Such cells likely synthesize high levels of ribosomes not solely to increase their size, but rather to maintain a high level of biosynthetic activity. Therefore, it is possible that the function of *ncl-1* can be thought of not simply as being a repressor of cell size, but more specifically as an inhibitor of the level of biosynthetic activity within a cell. Together, our results indicate that NCL-1 is a key molecule in the regulation of cell growth and ribosome synthesis.

Possible Mechanisms for ncl-1–mediated Regulation of Ribosome Synthesis and Cell Size

The mechanism by which ribosome synthesis is coupled to cell growth is unclear. It has been proposed that a feedback mechanism exists wherein the ratio of free ribosomes to polysomes is monitored. When this ratio becomes too high (i.e., there are many inactive ribosomes not engaged in translation), ribosomal RNA synthesis is downregulated, and when this ratio becomes too low (i.e., the majority of ribosomes are engaged) then ribosomal RNA synthesis is upregulated (for review see Nomura et al., 1984). In light of this, two models for the molecular function of *ncl-1* can be considered. The first is that *ncl-1* functions to inhibit translation. This would result in a decrease in polysomes and an increase in free ribosomes, which would lead to a decrease in rRNA transcription. The fact that *ncl-1* worms have more protein, and presumably a higher level of protein synthesis, than wild-type worms is consistent with this model. The second model is that *ncl-1* functions in sensing the ratio of free ribosomes to polysomes and directs the level of rRNA transcription. Finally, it is possible that although the majority of NCL-1 protein appears by immunocytochemistry to be cytoplasmic, some NCL-1 protein may be nuclear, and might act directly as a transcription factor to inhibit RNA polymerase I and III transcription.

The control of cell size is of clinical interest as many forms of human heart failure and kidney disease caused by diabetes are associated with enlarged cells (hypertrophy) in cardiac and renal tissues (for review see Hannan and Rothblum, 1995; Kurabayashi and Yazaki, 1996; Rabkin and Fervenza, 1996). In studies of cardiac hypertrophy, it has been found that ribosomal RNA synthesis increases (McDermott et al., 1989), consistent with the idea that increased cell size is correlated with an increased capacity for protein synthesis. Although the mechanism of this transcriptional upregulation has not been determined, it has been found that UBF (upstream binding factor, the RNA polymerase I transcriptional activator) becomes phosphorylated (Hershey et al., 1995), an event which is correlated with its activation (Voit et al., 1992). Likewise, ribosomal protein S6 becomes phosphorylated by S6 kinase (Takano et al., 1996); phosphorylation of S6 correlates with higher translation efficiency (Proud, 1996). It is possible that this results in an increase in rRNA transcription via the feedback mechanism discussed above. Thus far, there are no genetic systems available to study hypertrophy. As *ncl-1* mutants exhibit phenotypes characteristic of hypertrophy (increased cell size, increased steady-state rRNA, and increased rate of rRNA transcription), we propose that *ncl-1* provides a model genetic system in which to approach this problem of the regulation of hypertrophic growth.

NCL-1 Is Related in Sequence to Oncogenes Such as PML and May Share with Rb the Ability to Repress the Synthesis of Ribosomal RNAs

NCL-1 has B box zinc finger and coiled-coil motifs common to several proteins including PML, T18, and RFP (for review see Reddy et al., 1992). This similarity is intriguing in that these three genes were all identified as translocations that result in tumorigenesis. For instance, PML was found as a translocation resulting in a fusion protein between the zinc fingers and coiled-coil of PML and the retinoic acid receptor (RAR); the fusion protein PML–RAR is responsible for acute promyelocytic leukemia in humans (Borrow et al., 1990; de The et al., 1990; Kakizuka et al., 1991). Although the mechanism of transformation by the PML–RAR fusion protein is still unclear, PML alone may function normally as a growth suppressor since it has been shown to be able to inhibit transformation in cell culture (Mu et al., 1994). Because tumor cells often have enlarged nucleoli (Busch and Smetana, 1970; Derenzini and Trere, 1991), it is conceivable that these genes and *ncl-1* might have overlapping functions.

One other cancer related gene, the tumor suppressor Rb, is structurally unrelated but does share some common functions with *ncl-1*. Recent evidence suggests that, like *ncl-1* mutants, loss of Rb function may derepress transcription by RNA polymerase I and III (Cavanaugh et al., 1995; White et al., 1996). It is possible that one way in which tumor cells are able to achieve an increase in cell growth is by increasing their ability to synthesize proteins through mutation of a gene such as Rb that normally functions to repress RNA polymerase I and III transcription (for review see Nasmyth, 1996; White, 1997). Interestingly, it has been shown that chimeric mice containing Rb-deficient cells have enlarged cells in the liver and cerebellum (Williams et al., 1994), suggesting that Rb, like *ncl-1*, may be required to limit the size of cells. Furthermore, induction of cellular hypertrophy in cardiomyocytes leads to increased phosphorylation of Rb (Sadoshima et al., 1997). It will be interesting to learn if there is Rb in *C. elegans*, and if so, how it and *ncl-1* might function together to achieve the goal of negatively regulating cell size and ribosomal RNA synthesis. Conversely, it will be interesting to learn if there is a *ncl-1*-like gene in mammalian cells and whether or not its function is abrogated in tumor cells.

We thank our colleagues at Fred Hutchinson Cancer Research Center: B. Edgar, L. Moore, M. Morrison, S. Parkhurst, J. Priess, J. Roberts, L.B. Roth, and J. Stark for critical reading of the manuscript and D. Waring for helpful advice.

D.J. Frank was supported by a graduate fellowship from the National Science Foundation. This work was supported by a National Institutes of Health grant (GM48435-01A2) to M.B. Roth.

Received for publication 21 November 1997 and in revised form 21 January 1998.

References

Albertson, D.G. 1984. Formation of the first cleavage spindle in nematode embryos. *Dev. Biol.* 101:61–72.

Allo, S.N., P.J. McDermott, L.L. Carl, and H.E. Morgan. 1991. Phorbol ester stimulation of protein kinase C activity and ribosomal DNA transcription. *J. Biol. Chem.* 266:22003–22009.

Altman, P.L., and D.D. Katz 1976. Cell Biology. *FASEB (Fed. Am. Soc. Exp. Biol.)*, Bethesda, MD. 454 pp.

Altmann, G.G., and C.P. Leblond. 1982. Changes in the size and structure of the nucleolus of columnar cells during their migration from crypt base to villus top in rat jejunum. *J. Cell Sci.* 56:83–99.

Ausubel, F.M., R. Brent, R.R. Kingston, D.D. Moore, J.G. Seideman, J.A. Smith, and K. Struhl. 1987. Analysis of RNA by Northern Hybridization. *In* Current Protocols in Molecular Biology. Vol. 1. Wiley/Greene, New York. 4.9.1–4.9.4.

Borrow, J., A. Goddard, D. Sheer, and E. Solomon. 1990. Molecular analysis of acute promyelocytic leukaemia breakpoint cluster region on chromosome 17. *Science.* 249:1577–1580.

Brenner, S. 1974. The genetics of *Caenorhabditis elegans. Genetics.* 77:71–94.

Busch, H., and K. Smetana. 1970. The Nucleolus. Academic Press, New York. 626 pp.

Cavanaugh, A.H., W.M. Hempel, L.J. Taylor, V. Rogalsky, G. Todorov, and L.I. Rothblum. 1995. Activity of RNA polymerase I transcription factor UBF blocked by Rb gene product. *Nature.* 374:177–180.

Cluzeaud, F., J. Perennec, E. deAmoral, M. Willemin, and P.Y. Hatt. 1984. Myocardial cell nucleus in cardiac overloading in the rat. *Eur. Heart J.* 5:271–280.

Dalen, H., T. Saetersdal, and S. Odegarden. 1987. Some ultrastructural features of the myocardial cells in the hypertrophied human papillary muscle. *Virchows Arch. A Pathol. Anat. Histopathol.* 410:281–294.

Derenzini, M., and D. Trere. 1991. Importance of interphase nucleolar organizer regions in tumor pathology. *Virchows Arch. B Cell Pathol.* 61:1–8.

de The, H., C. Chomienne, M. Lanotte, L. Degos, and A. Dejean. 1990. The t(15;17) translocation of acute promyelocytic leukaemia fuses the retinoic acid receptor α gene to a novel transcribed locus. *Nature.* 347:558–561.

Dumont, J.N. 1972. Oogenesis in *Xenopus laevis* (Daudin) I. Stages of oocyte development in laboratory maintained animals. *J. Morphol.* 136:153–180.

Ellis, R.E., J.E. Sulston, and A.R. Coulson. 1986. The rDNA of *C. elegans*: sequence and structure. *Nucleic Acids Res.* 14:2345–2363.

Ferguson, K.C., P.J. Heid, and J.H. Rothman. 1996. The SL1 trans-spliced leader RNA performs an essenetial embryonic function in *Caenorhabditis elegans* that can also be supplied by SL2 RNA. *Genes Dev.* 10:1543–1556.

Files, J.G., and D. Hirsh. 1981. Ribosomal DNA of *Caenorhabditis elegans. J. Mol. Biol.* 149:223–240.

Fischetti, V.A., G.M. Landau, J.P. Schmidt, and P. Sellers. 1993. Identifying periodic occurrences of a template with applications to protein structure. *Inf. Proc. Lett.* 45:11–18.

Garber, M., S. Panchanathan, R.S. Fan, and D.L. Johnson. 1991. The phorbol ester, 12-O-tetradec specific transcription by RNA polymerase III in Drosophila Schneider cells. *J. Biol. Chem.* 266:20598–20601.

Guo, S., and K.J. Kemphues. 1995. par-1, a gene required for establishing polarity in *C. elegans* embryos, encodes a putative Ser/Thr kinase that is asymmetrically distributed. *Cell.* 81:611–620.

Hannan, R.D., and L.I. Rothblum. 1995. Regulation of ribosomal DNA transcription during neonatal cardiomyocyte hypertrophy. *Card. Res.* 30:501–510.

Harlow, E., and D. Lane. 1988. Antibodies: A Laboratory Manual. Cold Spring Harbor Laboratory Press, Cold Spring Harbor, NY. 726 pp.

Hatt, P.Y., P. Jouannot, J. Moravec, J. Perennec, and M. Laplace. 1978. Development and reversal of pressure-induced cardiac hypertrophy. Light and electron microscopic study in the rat under temporary aortic constriction. *Basic Res. Cardiol.* 73:405–421.

Hedgecock, E.M., and R.K. Herman. 1995. The ncl-1 gene and genetic mosaics of *Ceanorhabditis elegans. Genetics.* 141:989–1006.

Hershey, J.C., M. Hautmann, M.M. Thompson, L.I. Rothblum, T.A.J. Haystead, and G.K. Owens. 1995. Angiotensin II-induced hypertrophy of rat vascular smooth muscle is associated with increased 18S rRNA synthesis and phosphorylation of the rRNA transcription factor, upstream binding factor. *J. Biol. Chem.* 270:25096–25101.

Johnson, L.F., H.T. Abelson, H. Green, and S. Penman. 1974. Changes in RNA in relation to growth of the fibroblast. I. Amounts of mRNA, rRNA, and tRNA in resting and growing cells. *Cell.* 1:95–100.

Kakizuka, A., W.H. Miller, R.P. Umesono, S. Warrell, V.V.V.S. Frankel, E. Marty, E. Dmitrowsky, and R.M. Evans. 1991. Chromosomal translocation t(15;17) in human acute promyelocytic leukaemia fuses RARα with a novel putative transcription factor, PML. *Cell.* 66:663–674.

Kipreos, E.T., L.E. Lander, J.P. Wing, W.W. He, and E.M. Hedgecock. 1996. cul-1 is required for cell cycle exit in *C. elegans* and identifies a novel gene family. *Cell.* 85:829–839.

Kurabayashi, M., and Y. Yazaki. 1996. Molecular biology of heart disease synopsis of the pathophysiological basis of cardiac hypertrophy, familial hypertrophic cardiomyopathy, long QT syndrome and Marfan syndrome. *Int. Med.* 35:243–248.

Kurata, S., K. Koga, and B. Sakaguchi. 1978. Nucleolar size in parallel with ribosomal RNA synthesis at diapause termination in the eggs of Bombyx mori. *Chromosoma (Berl.).* 68:313–317.

Liebhaber, S.A., S. Wolf, and D. Schlessinger. 1978. Differences in rRNA metabolism of primary and SV40-transformed human fibroblasts. *Cell.* 13:121–127.

McDermott, P.J., L.I. Rothblum, D. Smith, and H.E. Morgan. 1989. Accelerated rates of ribosomal RNA synthesis during growth of contracting heart cells in culture. *J. Biol. Chem.* 264:18220–18227.

Melese, T., and Z. Xue. 1995. The nucleolus: an organelle formed by the act of building a ribosome. *Curr. Opin. Cell Biol.* 7:319–324.

Mello, C.C., J.M. Kramer, D. Stinchcomb, and V. Ambros. 1991. Efficient gene transfer in *C. elegans*: extrachromosomal maintenance and integration of

transforming sequences. *EMBO (Eur. Mol. Biol. Organ.) J.* 10:3959–3970.
Miller, L.M., D.A. Waring, and S.K. Kim. 1996. Mosaic analysis using a ncl-1 (+) extrachromosomal array reveals that lin-31 acts in the Pn.p cells during *Caenorhabditis elegans* vulval development. *Genetics.* 143:1181–1191.
Moss, T., and V.Y. Stefanovsky. 1995. Promotion and regulation of ribosomal transcription in eukaryotes by RNA polymerase I. *Prog. Nucleic Acid Res. Mol. Biol.* 50:25–66.
Mu, Z., K. Chin, J. Liu, G. Lozano, and K. Chang. 1994. PML, a growth suppressor disrupted in acute promyelocytic leukemia. *Mol. Cell. Biol.* 14:6858–6867.
Nasmyth, K. 1996. Another role rolls in. *Nature.* 382:28–29.
Nomura, M., R. Gourse, and G. Baughman 1984. Regulation of the synthesis of ribosomes and ribosomal components. *Annu. Rev. Biochem.* 53:75–117.
Perry, R.P. 1976. Processing of RNA. *Annu. Rev. Biochem.* 45:605–629.
Prescott, D.M. 1976. Reproduction of Eukaryotic Cells. Academic Press, New York, 177 pp.
Proud, C.G. 1996. p70 S6 kinase: an enigma with variations. *Trends Biochem. Sci.* 21:181–185.
Rabkin, R., and F.C. Fervenza. 1996. Renal hypertrophy and kidney disease in diabetes. *Diabetes/Metab. Rev.* 12:217–241.
Rakusan, K. 1984. Cardiac growth, maturation, and aging. *In* Growth of the Heart in Health and Disease. R. Zak, editor. Raven Press, New York, 131–164.
Reddy, B.A., L.D. Etkin, and P.S. Freemont. 1992. A novel zinc finger coiled-coil domain in a family of nuclear proteins. *Trends Biochem. Sci.* 17:344–345.
Roberts, S.B., S.W. Emmons, and G. Childs. 1989. Nucleotide sequences of *Caenorhabditis elegans* core histone genes. *J. Mol. Biol.* 206:567–577.
Sadoshima, J., H. Aoki, and S. Izumo. 1997. Angiotensin II and serum differentially regulate expression of cyclins, activity of cyclin-dependent kinases, and phosphorylation of retinoblastoma gene product in neonatal cardiac myocytes. *Circ. Res.* 80:228–241.
Schaffner, W., and C. Weissmann. 1973. A rapid, sensitive, and specific method for the determination of protein in dilute solution. *Anal. Biochem.* 56:502–514.
Schauer, I.E., and W.B. Wood. 1990. Early *C. elegans* embryos are transcriptionally active. *Development (Camb.).* 110:1303–1317.
Schmidt, T., P.S. Chen, and M. Pellegrini. 1985. The induction of ribosome biosynthesis in a nonmitotic secretory tissue. *J. Biol. Chem.* 260:7645–7650.
Seydoux, G., and A. Fire. 1994. Soma-germline asymmetry in the distributions of embryonic RNAs in *Caenorhabditis elegans. Development (Camb.).* 120: 2823–2834.
Sulston, J., Z. Du, D. Thomas, R. Wilson, L. Hillier, R. Staden, N. Halloran, P. Green, J. Thierry-Mieg, L. Qiu et al. 1992. The *C. elegans* genome sequencing project: a beginning. *Nature.* 356:37–41.
Takano, H., I. Komuro, Y. Zou, S. Kudoh, T. Yamazaki, and Y. Yazaki. 1996. Activation of p70 S6 protein kinase is necessary for angiotensin II-induced hypertrophy in neonatal rat cardiac myocytes. *FEBS (Fed. Eur. Biochem. Soc.) Lett.* 379:255–259.
Vallett, S.M., M. Brudnak, M. Pellegrini, and H.W. Weber. 1993. In vivo regulation of rRNA transcription occurs rapidly in nondividing and dividing Drosophila cells in response to a phorbol ester and serum. *Mol. Cell. Biol.* 13:928–933.
Voit, R., A. Schnapp, A. Kuhn, H. Rosenbauer, P. Hirschmann, H.G. Stunnenberg, and I. Grummt. 1992. The nucleolar transcription factor mUBF is phosphorylated by casein kinase II in the C-terminal hyperacidic tail which is essential for transactivation. *EMBO (Eur. Mol. Biol. Organ.) J.* 11:2211–2218.
White, J. 1988. The anatomy. *In* The Nematode *Caenorhabditis elegans.* W.B. Wood, editor. Cold Spring Harbor Laboratory Press, Cold Spring Harbor, NY. 81–122.
White, R.J. 1997. Regulation of RNA polymerases I and III by the retinoblastoma protein: a mechanism for growth control? *Trends Biochem. Sci. Soc.* 22:77–80.
White, R.J., D. Trouche, K. Martin, S.P. Jackson, and T. Kouzarides. 1996. Repression of RNA polymerase III transcription by the retinoblastoma protein. *Nature.* 382:88–90.
Williams, B.O., E.M. Schmitt, L. Remington, R.T. Bronson, D.M. Albert, R.A. Weinberg, and T. Jacks. 1994. Extensive contribution of Rb-deficient cells to adult chimeric mice with limited histopathological consequences. *EMBO (Eur. Mol. Biol. Organ.) J.* 13:4251–4259.
Wilson, E.B. 1896. The Cell in Development and Inheritance. Johnson Reprint Corporation, New York. 371 pp.
Wood, W.B. 1988. Embryology. *In* The Nematode Caenorhabditis elegans. W.B. Wood, editor. Cold Spring Harbor Laboratory Press, Cold Spring Harbor, NY. 215–241.